Original Article | Cardiovascular Imaging

eISSN 2005-8330
https://doi.org/10.3348/kjr.2023.0985
Korean J Radiol 2024;25(5):426-437

Korean Journal of Radiology
KJR

Light-Chain Cardiac Amyloidosis: Cardiac Magnetic Resonance for Assessing Response to Chemotherapy

Yubo Guo[1], Xiao Li[1], Yajuan Gao[2], Kaini Shen[2], Lu Lin[1], Jian Wang[1], Jian Cao[1], Zhuoli Zhang[3], Ke Wan[4], Xi Yang Zhou[5], Yucheng Chen[6], Long Jiang Zhang[5], Jian Li[2], Yining Wang[1]

[1]Department of Radiology, State Key Laboratory of Complex Severe and Rare Diseases, Peking Union Medical College Hospital, Chinese Academy of Medical Sciences and Peking Union Medical College, Beijing, China
[2]Department of Hematology, State Key Laboratory of Complex Severe and Rare Diseases, Peking Union Medical College Hospital, Chinese Academy of Medical Sciences and Peking Union Medical College, Beijing, China
[3]Department of Radiological Sciences, University of California, Irvine, CA, USA
[4]Department of Geriatrics and National Clinical Research Center for Geriatrics, West China Hospital, Sichuan University, Chengdu, China
[5]Department of Diagnostic Radiology, Jinling Hospital, Medical School of Nanjing University, Nanjing, China
[6]Department of Cardiology, West China Hospital, Sichuan University, Chengdu, China

Objective: Cardiac magnetic resonance (CMR) is a diagnostic tool that provides precise and reproducible information about cardiac structure, function, and tissue characterization, aiding in the monitoring of chemotherapy response in patients with light-chain cardiac amyloidosis (AL-CA). This study aimed to evaluate the feasibility of CMR in monitoring responses to chemotherapy in patients with AL-CA.

Materials and Methods: In this prospective study, we enrolled 111 patients with AL-CA (50.5% male; median age, 54 [interquartile range, 49–63] years). Patients underwent longitudinal monitoring using biomarkers and CMR imaging. At follow-up after chemotherapy, patients were categorized into superior and inferior response groups based on their hematological and cardiac laboratory responses to chemotherapy. Changes in CMR findings across therapies and differences between response groups were analyzed.

Results: Following chemotherapy (before vs. after), there were significant increases in myocardial T2 (43.6 ± 3.5 ms vs. 44.6 ± 4.1 ms; $P = 0.008$), recovery in right ventricular (RV) longitudinal strain (median of -9.6% vs. -11.7%; $P = 0.031$), and decrease in RV extracellular volume fraction (ECV) (median of 53.9% vs. 51.6%; $P = 0.048$). These changes were more pronounced in the superior-response group. Patients with superior cardiac laboratory response showed significantly greater reductions in RV ECV (-2.9% [interquartile range, -8.7%–1.1%] vs. 1.7% [-5.5%–7.1%]; $P = 0.017$) and left ventricular ECV (-2.0% [-6.0%–1.3%] vs. 2.0% [-3.0%–5.0%]; $P = 0.01$) compared with those with inferior response.

Conclusion: Cardiac amyloid deposition can regress following chemotherapy in patients with AL-CA, particularly showing more prominent regression, possibly earlier, in the RV. CMR emerges as an effective tool for monitoring associated tissue characteristics and ventricular functional recovery in patients with AL-CA undergoing chemotherapy, thereby supporting its utility in treatment response assessment.

Keywords: Amyloidosis; Chemotherapy; Cardiac magnetic resonance; Tissue characterization; Longitudinal strain

Received: Octoer 9, 2023 **Revised:** February 29, 2024 **Accepted:** March 18, 2024

Corresponding author: Yining Wang, MD, Department of Radiology, State Key Laboratory of Complex Severe and Rare Diseases, Peking Union Medical College Hospital, Chinese Academy of Medical Sciences and Peking Union Medical College, No.1, Shuaifuyuan, Dongcheng District, Beijing 100730, China
• E-mail: wangyining@pumch.cn
Corresponding author: Jian Li, MD, Department of Hematology, State Key Laboratory of Complex Severe and Rare Diseases, Peking Union Medical College Hospital, Chinese Academy of Medical Sciences and Peking Union Medical College, No.1, Shuaifuyuan, Dongcheng District, Beijing 100730, China
• E-mail: lijian@pumch.cn

Korean Journal of Radiology
KJR

INTRODUCTION

Light-chain (AL) amyloidosis is a fatal disease characterized by the accumulation of misfolded immunoglobulin light chains produced by clonal plasma cells in the bone marrow, resulting in tissue damage in various organs. Among these, the severity of cardiac involvement is a key determinant of prognosis [1]. AL cardiac amyloidosis (AL-CA) is caused by dual insults of amyloid infiltration and AL myotoxicity [2], which can induce sudden cardiac death or acute heart failure. Untreated AL-CA patients with heart failure face a median survival of approximately six months [3]; however, advancements in new chemotherapeutics have positively impacted patient prognosis [4].

Biomarkers offer prognostic significance and determine treatment response [5]. Hematological responses are the first step in treatment and prerequisites for cardiac responses. Serum free light chain (FLC) levels are robust biomarkers of hematological responses. Currently, the most commonly used cardiac response assessments rely on surrogates, including N-terminal pro-B-type natriuretic peptide (NT-proBNP), cardiac troponin, and echocardiographic parameters. However, none of these response assessments directly quantify disease burden, underscoring the urgent need to identify biomarkers to assess treatment responses at the myocardial level.

Cardiac magnetic resonance (CMR) emerges as the preferred imaging modality for diagnosing cardiomyopathy. CMR is an excellent tool for noninvasive tissue characterization because it can visualize and facilitate the measurement of myocardial lesions using late gadolinium enhancement (LGE) or T1 and T2 mapping. In patients with AL-CA, the pattern of LGE and elevation in native T1 and extracellular volume fraction (ECV) are considered biomarkers of amyloid infiltration, facilitating early disease detection [6,7]. Moreover, ECV functions as a robust predictor of mortality and adds incremental value to known prognostic factors [8]. Although echocardiography is commonly used to assess ventricular function based on volumetric measures, image quality can be highly variable among patients, and defining the endocardium on long-axis images can be challenging. However, CMR is considered the gold standard for assessing left ventricular (LV) and right ventricular (RV) volumetric and strain imaging. Its ability to provide precise and reproducible quantitative information about cardiac structure, function, and tissue characterization obtained makes it invaluable for accurately assessing changes following treatment in patients with AL-CA.

This prospective multicenter study aimed to evaluate the feasibility of CMR for monitoring responses to chemotherapy and changes in myocardial composition in patients with AL-CA.

MATERIALS AND METHODS

Patient Population

This study was approved by the Institutional Ethics Committee of the Peking Union Medical College Hospital (Beijing, China). Patients diagnosed with AL amyloidosis were recruited between December 2013 and July 2021 after providing written informed consent from three hospitals: Peking Union Medical College Hospital (Beijing, China), Jinling Hospital (Nanjing, China), and West China Hospital (Chengdu, China). Before enrollment, AL amyloidosis was diagnosed by biopsy, showing amyloid deposition with amyloid typing by immunohistochemistry or mass spectroscopy. Cardiac involvement was defined as an NT-proBNP level > 332 pg/mL and LV mean wall thickness > 12 mm in the absence of hypertension or other potential causes of LV hypertrophy. Patients without cardiac involvement or with contraindications to MRI (claustrophobia, metallic implants, estimated glomerular filtration rate < 30 mL/min/1.73 m^2) were excluded from the study. Mayo staging utilized the European modification of the Mayo 2004 staging assessment, incorporating the assessment of NT-proBNP and cardiac troponin I or T levels for survival prediction [9].

We prospectively enrolled 111 patients who underwent comprehensive assessments, including biomarkers and CMR, before therapy and at a median follow-up of 12 months (interquartile range [IQR], 10–16 months) after the completion of nine cycles of chemotherapy (Fig. 1). All patients received standard bortezomib- or melphalan-based chemotherapy directed toward abnormal plasma cell clones. Patients were categorized based on previously published response criteria [1,10]. Hematologic responses were graded as follows: 1) complete response to normal FLC levels, normal kappa/lambda ratio, and negative serum and urine immunofixation, 2) very good partial response, difference between involved and uninvolved FLC (dFLC) reduced to < 40 mg/L, and 3) partial response, dFLC reduced by > 50%. For cardiac laboratory responses, complete response, very good partial response, partial response, and no response were defined as NT-proBNP less than or equal to 400 pg/mL, greater than 60% reduction in NT-proBNP, 31% to 60% reduction in NT-proBNP, and less than 30% reduction in NT-proBNP, respectively. Patients achieving complete or very good

 https://doi.org/10.3348/kjr.2023.0985

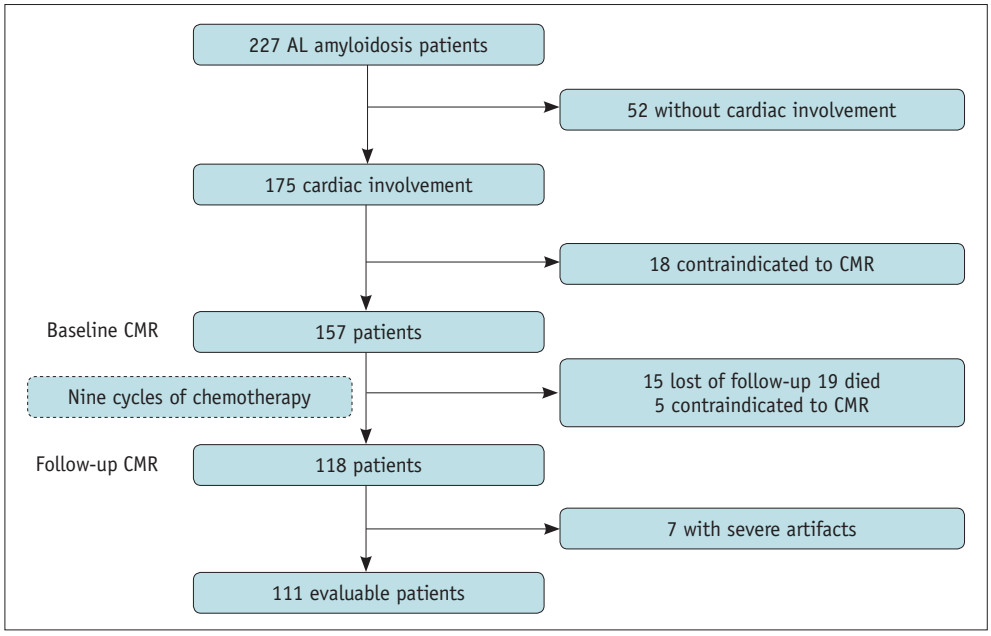

Fig. 1. Flow diagram illustrating patient inclusion. AL = light-chain, CMR = cardiac magnetic resonance

partial response were categorized into the superior response group, whereas the remaining patients were categorized into the inferior response group.

CMR Protocol

CMR imaging was performed utilizing 3T whole-body scanners (MAGNETOM Skyra or Trio, Siemens Healthcare, Erlangen, Germany) equipped with an 18-element body matrix coil and a 32-element spine array coil for image acquisition. Electrocardiographic gating and breath-holding were employed in the imaging process.

Cine images were acquired using an electrocardiography-gated balanced steady-state free precession sequence (bSSFP) in two-, three-, and four-chamber long-axis as well as short-axis views (repetition time/echo time/flip angle, 3.3 ms/1.43 ms/55°–70°; voxel size, 1.6 x 1.6 x 6.0 mm^3; temporal resolution, 45.6 msec; bandwidth, 962 Hz/pixel). Native and 15–20 min post-contrast T1 maps were acquired using a modified Look-Locker inversion-recovery sequence in identical imaging locations, including a four-chamber long-axis view and basal-, mid-, and apical-ventricular short-axis views (repetition time/echo time/flip angle, 2.7 ms/1.12 ms/20°; voxel size, 1.4 x 1.4 x 8.0 mm^3). Acquisition schemas 5(3)3 and 4(1)3(1)2 were used for pre- and post-contrast T1 mapping, respectively. T2 mapping was acquired using a T2-prepared single-shot bSSFP sequence with slice positions matching the T1 mapping images (repetition time/echo time/flip angle, 2.4 ms/1.0 ms/70°; field of view, 320–340 x 262–278 mm^2; slice thickness, 8 mm; bandwidth, 1093 Hz/pixel; GeneRalized Autocalibrating Partially Parallel Acquisitions acceleration factor, 2). LGE images were collected using a phase-sensitive inversion-recovery gradient-echo pulse sequence (repetition time/echo time/flip angle, 5.2 ms/1.96 ms/20°; voxel size, 1.4 x 1.4 x 8.0 mm^3) in the same views as the cine images 10 min after intravenous gadolinium injection (0.15 mmol/kg body weight) [11].

CMR Image Analysis

Utilizing clinical data, CMR image analysis included measuring cardiac function, ventricular strain, native T1, ECV, and T2, which were semi-automatically measured using cvi42 software (version 5.12; Circle Cardiovascular Imaging, Calgary, Canada) by one observer (Y.G., with 4 years of CMR experience). Standard parameters of cardiac structure and function were calculated by contouring the endocardium and epicardium on long- and short-axis cine images during the end-systolic and end-diastolic phases. Global and segmental strain parameters were automatically calculated using the software, encompassing radial and circumferential strains from short-axis cine slices and longitudinal strain (LS) from three long-axis cine slices. Endocardial and epicardial borders were selected during the end-diastole phase, and subsequent phase imaging borders were automatically generated. LV native T1 and T2 values were measured on three short-axis stacks by contouring

https://doi.org/10.3348/kjr.2023.0985

Korean Journal of Radiology
KJR

the endocardium and epicardium with stable test-retest reproducibility [12]. An offset of 5% was applied to the contours to prevent signal contamination. RV T1 values were derived from manually drawn regions of interest within the diaphragmatic wall, ensuring avoidance of contact with the blood pool or epicardial fat (Fig. 2) [13]. Local normal ranges were determined as 1295.0 ± 36.2 ms for T1 and 40.3 ± 2.3 ms for T2 [14]. ECV values were obtained from pre- and post-contrast T1 map indexes of hematocrit. Relative intracellular volume was calculated using the formula [1 – ECV]; "total intracellular mass" was calculated with the formula [relative intracellular volume x total LV myocardial volume x myocardial density], using the well-known myocardial density value of 1.055 g/mL for human; and "total extracellular mass" with the formula [ECV x total LV myocardial volume x myocardial density], using a different myocardial density value of 1.38 g/mL for extracellular infiltrative disease, as described in the previous work [15]. The LV LGE patterns were graded according to the Moon criteria as follows: 1 = none, 2 = subendocardial, and 3 = transmural [6].

Statistical Analysis

Statistical analyses were performed using IBM SPSS Statistics for Windows version 26 (IBM Corp., Armonk, NY, USA). Continuous variables are presented as mean ± standard deviation or median (IQR) for normally and non-normally

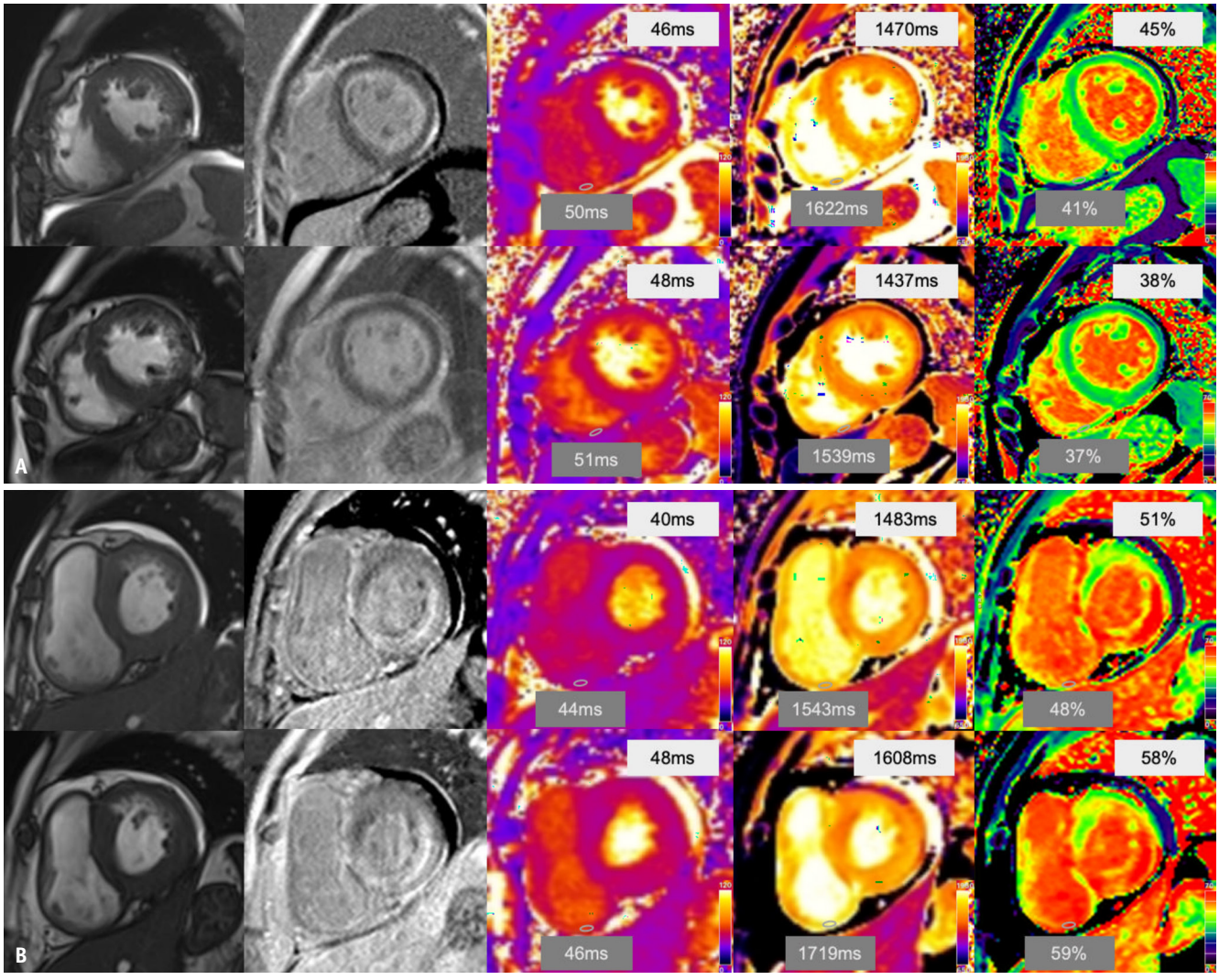

Fig. 2. Regression and progression in patients with AL-CA. **A, B:** Patient showing disease regression **(A)**, patient showing disease progression **(B)**. Serial cardiac magnetic resonance scans with cine, late gadolinium enhancement, T2, native T1, and extracellular volume fraction at baseline (top) and at follow-up (bottom) showing cardiac response. Left ventricle myocardial tissue characterization was derived from short axis stacks by contouring the endocardium and epicardium. Meanwhile, right ventricle myocardial tissue characterization was derived from region of interest drawn within the diaphragmatic wall. AL-CA = light-chain cardiac amyloidosis

https://doi.org/10.3348/kjr.2023.0985

distributed data, respectively. Categorical variables are expressed as absolute numbers and percentages. Continuous variables at baseline and follow-up were compared using the paired *t*-test or Wilcoxon test, and categorical variables were compared using the chi-square test. Comparisons between the response groups were performed using an independent *t*-test for normal data or Wilcoxon test for nonparametric data. All reported *P*-values were two-sided, with a significance level at < 0.05.

RESULTS

Patient Characteristics

In total, 222 CMRs scans were performed in 111 patients (50.5% male; median age, 54 years [IQR, 49–63 years]) before and after treatment. Among them, 108 received bortezomib-based chemotherapy, and three received melphalan-based chemotherapy. Follow-up scans were obtained approximately 12 months after treatment (IQR, 10–16 months). Hematologic responses included complete response in 66 (59.5%) patients, very good partial response in 27 (24.3%), partial response in 9 (8.1%), no response in 5 (4.5%), and progression in 4 (3.6%). Patients achieving complete or very good partial responses were categorized into the superior hematological response group (n = 93), whereas the remaining patients were categorized into the inferior hematological response group (n = 18). Cardiac laboratory responses were distributed as follows: complete response, 32 patients (28.8%); very good partial response, 27 patients (24.3%); partial response, 12 patients (10.8%); and no response, 40 patients (36.0%). Patients achieving complete or very good partial response were categorized into the superior cardiac laboratory response group (n = 59), and the remaining patients were categorized into the inferior cardiac laboratory response group (n = 52). Among those with superior hematologic response, 54 (58.1%) patients achieved superior cardiac laboratory response; among those with inferior hematologic response, 13 (72.2%) patients had inferior cardiac laboratory response. The baseline characteristics of the study groups are summarized in Table 1 and Supplementary Table 1.

The Ability of CMR to Track Changes in AL-CA

Following treatment, there was an overall reduction in dFLC, cardiac troponin I, and NT-proBNP levels. Significant ventricular enlargement was observed, as evidenced by increases in LV end-diastolic volume index (EDVi) (P < 0.001),

Table 1. Baseline characteristics of study cohort

Characteristic	All patients (n = 111)	Hematologic response		*P*	Cardiac laboratory response		*P*
		Superior response (n = 93)	Inferior response (n = 18)		Superior response (n = 59)	Inferior response (n = 52)	
Sex, male	56 (50.5)	50 (53.8)	6 (33.3)	0.113	30 (50.8)	26 (50.0)	0.929
Age, yr	54.0 [49.0–63.0]	54.0 [49.0–62.5]	51.5 [46.0–65.3]	0.628	57.0 [49.0–63.0]	52.0 [47.3–58.0]	0.087
NYHA functional class ≥ II	84 (75.7)	71 (76.3)	13 (72.2)	0.942	42 (71.2)	42 (80.8)	0.240
Mayo cardiac stage ≥ II	96 (86.5)	83 (92.1)	13 (72.2)	0.119	48 (81.4)	48 (92.3)	0.092
Presenting κ, mg/L	12.2 [8.6–23.4]	13.0 [9.00–23.0]	8.8 [6.5–99.5]	0.256	14.1 [8.9–43.1]	9.5 [6.7–12.7]	0.032
Presenting λ, mg/L	176.3 [50.7–282.5]	166.2 [79.9–282.5]	201.8 [9.2–277.5]	0.527	166.2 [25.2–282.9]	201.8 [81.9–229.2]	0.966
Abnormal κ/λ ratio	0.064 [0.033–0.141]	0.079 [0.035–0.139]	0.036 [0.023–11.437]	0.386	0.079 [0.033–2.992]	0.041 [0.032–0.113]	0.302
dFLC, mg/L	180.5 [94.7–305.1]	174.0 [95.9–321.2]	202.3 [80.6–283.1]	0.761	228.7 [85.8–422.4]	147.7 [97.4–234.3]	0.055
cTnI, μg/L	0.064 [0.030–0.130]	0.064 [0.030–0.145]	0.055 [0.024–0.102]	0.390	0.072 [0.020–0.173]	0.049 [0.031–0.107]	0.469
NT-proBNP, pg/mL	1620 [521–4313]	1620 [566–4536]	1547 [219–3214]	0.139	1441 [414–4706]	1734 [627–3350]	0.981
eGFR, mL/min/1.73 m^2	87.1 [69.8–102.8]	82.2 [67.2–99.7]	103.5 [93.2–122.2]	0.009	81.7 [66.3–103.2]	90.3 [86.5–98.9]	0.322
Creatinine, mmol/L	76.0 [60.0–93.0]	78.5 [65.5–97.0]	58.0 [58.0–67.0]	0.010	78.0 [63.8–98.3]	65.0 [58.0–77.5]	0.086
Hematocrit, %	40.6 [38.2–43.6]	40.6 [38.2–43.7]	41.5 [37.1–44.8]	0.901	40.5 [36.0–43.6]	40.8 [38.7–43.8]	0.577

Values are number (percentage) or median [interquartile range].
NYHA = New York Heart Association, dFLC = difference between involved and uninvolved free light chains, cTnI = cardiac troponin I, NT-proBNP = N-terminal pro-B-type natriuretic peptide, eGFR = estimated glomerular filtration rate

https://doi.org/10.3348/kjr.2023.0985

Korean Journal of Radiology
KJR

LV end-systolic volume index (ESVi) ($P < 0.001$), RV EDVi ($P = 0.001$), and RV ESVi ($P = 0.016$). The increase in EDVi surpassed that of ESVi, accompanied by an increase in the LV stroke volume index (SVi) ($P < 0.001$) and RV SVi ($P = 0.008$). RV LS ($P = 0.031$) and basal segmental LS ($P = 0.068$) showed improvement after treatment. LV mass significantly elevated ($P = 0.008$), with a decreasing trend in total extracellular mass and an increasing trend in total intracellular mass. RV ECV, reflecting amyloid deposition, significantly decreased after chemotherapy ($P = 0.048$). However, native LV T1 ($P = 0.337$) and ECV ($P = 0.272$) did not significantly decreases from baseline to follow-up in the overall population. Myocardial T2 values were significantly elevated after treatment ($P = 0.008$), with higher values representing higher free water content and myocardial edema. Table 2 and Figure 3 show the pre- and post-treatment serum biomarkers and CMR parameters, respectively.

The Ability of CMR to Assess Responses in AL-CA

We evaluated CMR parameters based on the degree of hematological and cardiac laboratory responses. Patients achieving a superior hematologic response showed greater improvements in RV CMR parameters, including RV SVi ($P = 0.007$), RV ejection fraction ($P = 0.009$), RV LS ($P = 0.082$), and RV ECV ($P = 0.091$) (Fig. 4A, B). Among the cardiac laboratory response groups, patients with a superior cardiac response showed a more significant decrease in LV myocardial T1 ($P = 0.047$) and ECV ($P = 0.01$) (Fig. 4C, D). LV mass ($P = 0.003$) and total extracellular mass ($P = 0.007$) were significantly lower in patients with a superior cardiac response. Similarly, there was a more significant decrease in RV ECV among patients with a superior cardiac response ($P = 0.017$). Most other measures of cardiac structure, function, and myocardial tissue characteristics did not differ significant between the groups (Table 3).

DISCUSSION

In this longitudinal multicenter study, we delineated the imaging biomarker trajectory of AL-CA after treatment. Our findings underscored the efficacy of CMR in monitoring AL-CA. Specifically, we found that CMR could provide valuable information regarding variations in tissue characterization and changes in ventricular function. CMR has the potential to improve our understanding of AL-CA and its treatment response.

Monitoring treatment responses in patients involves two aspects: 1) hematologic response using serologic markers, and 2) organ response based on cardiac function. Deeper hematological responses were more likely to contribute to cardiac responses. Accurate assessment of changes in cardiac involvement is crucial for treatment modulation; however, this assessment remains suboptimal. The present study focused on monitoring the longitudinal cardiac amyloid load using advanced CMR, incorporating parameters from the left and right ventricles.

T1 mapping enables the measurement of extracellular amyloid deposition in AL-CA [16]. We observed that ECV and native T1 tended to decrease after treatment, indicating a reduction in the amyloid burden at the individual level. Furthermore, this decrease varied between the response groups. Specifically, the RV ECV decreased upon achieving a hematologic response, and subsequently, the LV ECV decreased after achieving a cardiac response. Longitudinal data supported a causal relationship between changes in ECV and treatment. Our findings are consistent with those of recent studies, where the reduction in ECV and native T1 provided compelling evidence of cardiac amyloid regression [17-19]. The balance between amyloid accumulation and clearance can be altered by halting or slowing amyloid generation. T1 mapping allows the monitoring of myocardial amyloid regression after anti-plasma cell therapy and distinguishing responses to treatment.

RV amyloid infiltration is known to occur in the later stages of AL-CA compared to LV amyloid infiltration [20]; however, this pattern seems to reverse during amyloid elimination. Amyloid deposition typically initiates in the sub-endocardium [6], mainly affecting longitudinal muscle fibers [21]. Patients did not show functional improvement in LV LS after induction chemotherapy but subsequently experienced LV LS improvement after achieving a complete response at 12 months [22]. We observed that RV LS improved as RV ECV decreased after successful treatment, and this regression was more pronounced in the superior hematological response group. This suggests that the sensitivity of LS as a functional marker allows immediate assessment of treatment effects. The improvement in LS was likely due to reduced proteotoxic damage to cardiac myocytes, as the amyloid burden was reduced. Upon achieving a hematologic response, serum FLC levels normalize, and RV systolic function gradually recurpates.

The standard therapy for AL-CA targets abnormal plasma cell clones to eradicate monoclonal light chain-producing clonal plasma cells, leading to a decrease in light chain

 https://doi.org/10.3348/kjr.2023.0985

production. Evidence suggests that amyloid clearance can occur when their precursors are inhibited, potentially facilitating cardiac responses. In this process, the recovery of the right ventricle following chemotherapy was more prominent and probably earlier than that of left ventricle.

Cuddy et al. [23] reported higher myocardial T2 values

Table 2. Comparison between before and after chemotherapy

Parameter	Before	After	*P*
Presenting κ, mg/L	12.2 (8.6–23.4)	12.4 (9.3–18.3)	0.095
Presenting λ, mg/L	176.3 (50.7–282.5)	20.1 (12.8–26.0)	< 0.001
Abnormal κ/λ ratio	0.064 (0.033–0.141)	0.740 (0.508–0.853)	0.035
dFLC, mg/L	180.5 (94.7–305.1)	8.5 (2.7–19.8)	< 0.001
cTnI, μg/L	0.064 (0.030–0.130)	0.027 (0.017–0.050)	< 0.001
NT-proBNP, pg/mL	1620 (521–4313)	688 (302–2042)	< 0.001
eGFR, mL/min/1.73 m^2	87.1 (69.8–102.8)	80.4 (63.6–96.8)	0.064
Creatinine, mmol/L	76.0 (60.0–93.0)	80.0 (69.0–101.8)	0.167
Hematocrit, %	40.6 (38.2–43.6)	39.4 (35.3–43.0)	0.010
LGE	3 (2–3)	3 (2–3)	0.655
T2, ms	43.6 ± 3.5	44.6 ± 4.1	0.008
LV native T1, ms	1454.0 (1387.0–1506.0)	1446.0 (1369.0–1504.0)	0.337
LV ECV, %	48.0 (40.0–51.7)	46.0 (37.9–53.0)	0.272
Relative intracellular volume	0.534 ± 0.086	0.546 ± 0.098	0.177
Total extracellular mass, g	51.2 (29.8–74.2)	48.0 (29.6–67.6)	0.739
Total intracellular mass, g	40.1 (33.4–53.7)	41.3 (32.6–52.8)	0.123
LV massi, g/m^2	72.7 (54.3–102.0)	75.8 (55.9–108.9)	0.008
LV EDVi, mL/m^2	77.3 ± 30.3	87.7 ± 36.0	< 0.001
LV ESVi, mL/m^2	29.2 (21.8–41.7)	32.1 (24.2–50.3)	< 0.001
LV SVi, mL/m^2	40.0 (32.5–49.0)	44.2 (37.2–52.8)	< 0.001
Left atrial area, cm^2	55.3 (39.9–80.5)	55.9 (40.7–74.1)	0.794
LV EF, %	58.2 (49.5–65.2)	57.3 (50.5–64.3)	0.529
LV circumferential strain, %	-16.9 (-19.3–-13.7)	-16.7 (-19.2–-14.2)	0.517
LV longitudinal strain, %	-13.1 (-15.8–-8.7)	-13.7 (-16.7–-10.2)	0.068
LV radial strain, %	19.6 (12.7–26.1)	19.9 (14.0–28.2)	0.149
LV basal segmental circumferential strain, %	-15.6 ± 4.5	-15.4 ± 4.0	0.489
LV basal segmental longitudinal strain, %	-8.3 (-11.3–-5.5)	-8.4 (-10.8–-6.1)	0.501
LV basal segmental radial strain, %	27.1 ± 17.3	29.1 ± 17.8	0.106
RV native T1, ms	1559.0 (1483.0–1643.0)	1496.0 (1496.0–1623.0)	0.424
RV ECV, %	53.9 (46.4–62.4)	51.6 (47.2–58.7)	0.048
RV massi, g/m^2	17.7 (13.8–22.7)	18.2 (14.2–21.5)	0.297
RV EDVi, mL/m^2	69.7 ± 25.4	76.5 ± 28.9	0.001
RV ESVi, mL/m^2	32.1 (22.3–42.3)	32.4 (24.3–41.3)	0.016
RV SVi, mL/m^2	32.0 (27.5–41.6)	36.7 (28.9–41.7)	0.008
Right atrial area, cm^2	54.8 (36.5–73.7)	53.6 (42.8–69.6)	0.674
RV EF, %	52.3 (45.2–59.9)	54.0 (45.3–60.9)	0.195
RV circumferential strain, %	-12.8 (-16.1–-10.9)	-13.9 (-16.6–-11.0)	0.186
RV longitudinal strain, %	-9.6 (-13.5–-7.0)	-11.7 (-14.1–-8.8)	0.031
RV radial strain, %	32.4 (21.7–44.3)	34.9 (26.1–50.5)	0.140
RV basal segmental circumferential strain, %	-7.6 (-10.0–-4.8)	-7.8 (-10.2–-4.0)	0.803
RV basal segmental longitudinal strain, %	-9.7 (-13.3–-5.7)	-10.8 (-14.9–-5.9)	0.068
RV basal segmental radial strain, %	44.5 (28.8–79.1)	53.6 (34.5–75.8)	0.240

Values are presented as mean ± standard deviation or median (interquartile range).
dFLC = difference between involved and uninvolved free light chains, cTnI = cardiac troponin I, NT-proBNP = N-terminal pro–B-type natriuretic peptide, eGFR = estimated glomerular filtration rate, LGE = late gadolinium enhancement, LV = left ventricle, ECV = extracellular volume fraction, massi = mass index, EDVi = end-diastolic volume index, ESVi = end-systolic volume index, SVi = stroke volume index, EF = ejection fraction, RV = right ventricle

https://doi.org/10.3348/kjr.2023.0985

Korean Journal of Radiology
KJR

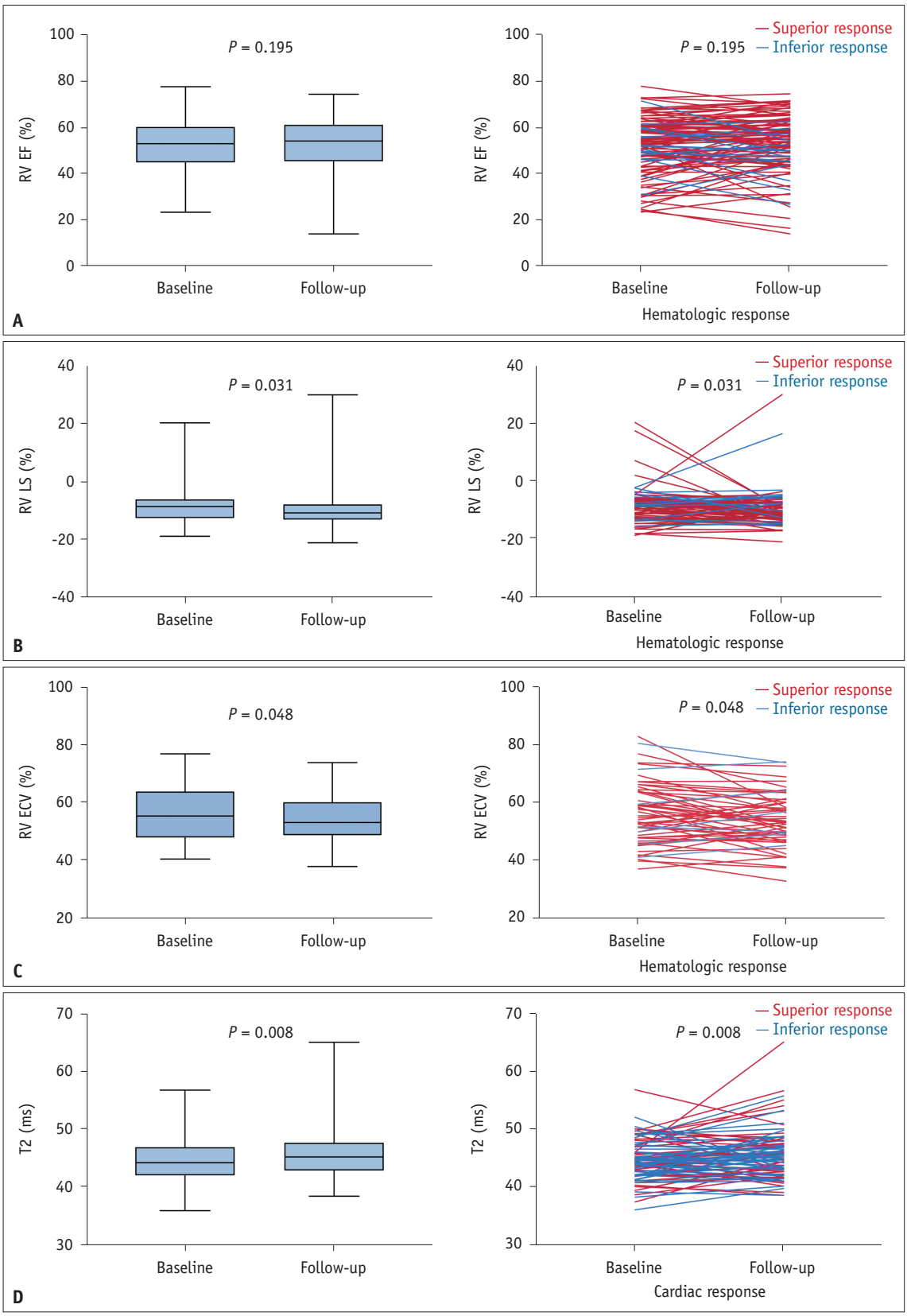

Fig. 3. Cardiac magnetic resonance in tracking changes. **A-D:** Changes observed in RV EF **(A)**, RV LS **(B)**, RV ECV **(C)**, and myocardial T2 value **(D)** of patients with light-chain cardiac amyloidosis following treatment. RV = right ventricle, EF = ejection fraction, LS = longitudinal strain, ECV = extracellular volume fraction

https://doi.org/10.3348/kjr.2023.0985

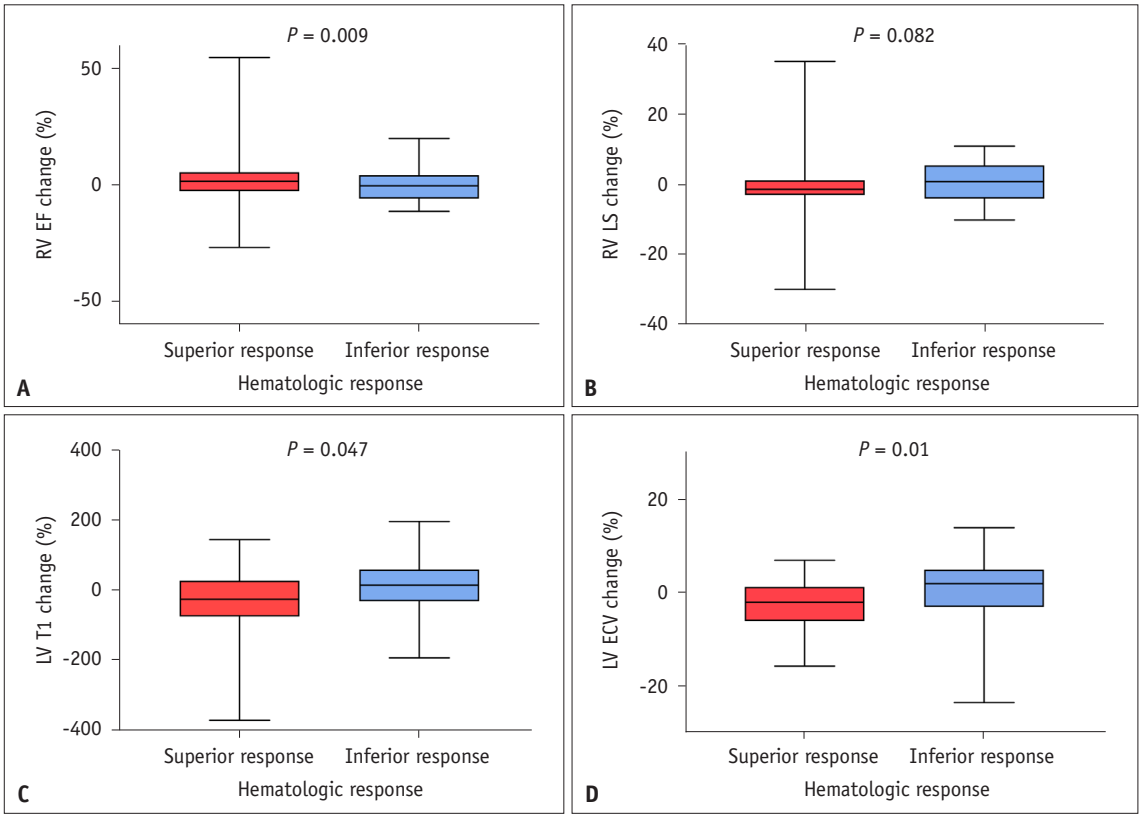

Fig. 4. Cardiac magnetic resonance in assessing responses. **A-D:** Changes observed in RV EF **(A)** and RV LS **(B)** in the hematologic response groups and changes in LV native T1 **(C)** and LV ECV **(D)** in the cardiac laboratory response group of light-chain cardiac amyloidosis patients following treatment. RV = right ventricle, EF = ejection fraction, LS = longitudinal strain, LV = left ventricle, ECV = extracellular volume fraction

in patients with hematologic remission than in those with active AL-CA, implying that T2 elevation occurred after chemotherapy. The present study confirmed the elevation of myocardial T2 levels after chemotherapy in a larger prospective cohort, with no significant differences between the response groups. Myocardial T2 elevation during the active phase is attributed to amyloid myotoxicity, leading to myocyte swelling and intracellular edema. T2 levels increased, rather than decreased, with treatment, which may indicate pseudo-progression due to superimposed proteasome inhibitor-related cardiotoxicity in the short term [24,25]. The rollback of myocardial T2 might be observed at further subsequent follows-up after chemotherapy. Additionally, an emerging treatment directly targeting amyloid deposits is in advanced stages of development and is likely to be applied to AL-CA in the next few years [26], potentially leading to more rapid and sustained organ responses.

This study had several limitations. First, the considerable mortality associated with AL-CA resulted in a survival bias in the available patient population, and follow-up enhanced CMR was contraindicated in some patients with inferior responses due to renal insufficiency. Second, responses to treatment were assessed at a short-term follow-up of one year. Future longitudinal studies using serial data to explore long-term changes would provide more comprehensive insights. Third, it is optimal to use endomyocardial pathology data to verify hypothetical theories. However, endocardial biopsy is too invasive to be justified as a follow-up procedure, particularly in patients with superior responses. Multimodal imaging integrating positron emission tomography, which directly images amyloid deposits, has the potential to detect pathological changes [27]. These limitations highlight the need for further research to address these issues and improve the assessment and management of patients with AL-CA.

In conclusion, advanced CMR methods allow noninvasive monitoring of initial changes in response to chemotherapy in patients with AL-CA. Notably, the LS was identified as a sensitive functional marker. Meanwhile, T1 mapping with ECV measurement could effectively track myocardial amyloid burden, revealing that recovery of the right ventricle

https://doi.org/10.3348/kjr.2023.0985

Korean Journal of Radiology
KJR

Table 3. Changes in serum biomarkers and CMR parameters according to response groups

Parameter	Hematologic response			Cardiac laboratory response		
	Superior response (n = 93)	Inferior response (n = 18)	*P*	Superior response (n = 59)	Inferior response (n = 52)	*P*
Follow-up, m	12.4 (10.3–16.5)	13.0 (10.2–14.7)	0.794	13.1 (11.4–16.0)	11.0 (9.8–16.0)	0.218
Changes in serum biomarkers						
dFLC, mg/L	-169.0 (-317.7–-85.7)	-114.2 (-186.3–-4.8)	0.024	-222.0 (-416.7–-80.8)	-112.5 (-201.9–-71.4)	0.019
cTnI, μg/L	-0.035 (-0.112–-0.003)	-0.011 (-0.041–0.022)	0.036	-0.045 (-0.145–-0.006)	-0.020 (-0.053–0.009)	0.003
NT-proBNP, pg/mL	-548 (-2482–-25)	113 (-375–1448)	0.001	-1070 (-3791–-306)	-14 (-443–883)	< 0.001
Hematocrit, %	-1.7 (-5.6–1.2)	-2.5 (-6.6–2.4)	0.950	-1.5 (-5.8–3.1)	-4.5 (-5.6–-0.7)	0.146
Changes in CMR parameters						
LGE	0 (0–0)	0 (0–0)	0.841	0 (0–0)	0 (0–0)	0.586
T2, ms	1.1 ± 3.9	0.4 ± 2.0	0.377	1.5 ± 4.3	0.5 ± 2.9	0.910
LV native T1, ms	-9.2 (-60.0–44.0)	2.0 (-27.3–66.3)	0.270	-25.6 (-75.0–27.0)	14.5 (-32.0–58.8)	0.047
LV ECV, %	-0.3 (-6.0–3.0)	1.0 (-1.0–2.5)	0.532	-2.0 (-6.0–1.3)	2.0 (-3.0–5.0)	0.010
Relative intracellular volume	0.011 ± 0.067	-0.003 ± 0.047	0.452	2.5 ± 5.3	-1.0 ± 7.2	0.007
Total extracellular mass, g	-0.7 (-6.8–7.7)	2.4 (-6.2–6.6)	0.901	-2.3 (-8.3–2.9)	4.4 (-5.9–11.3)	0.007
Total intracellular mass, g	1.6 (-3.1–8.1)	-0.5 (-5.3–6.6)	0.531	1.7 (-2.0–6.5)	1.5 (-4.6–13.7)	0.574
LV massi, g/m^2	1.3 (-4.1–9.0)	5.3 (0.2–11.0)	0.600	0.3 (-4.9–9.0)	4.2 (-1.6–10.5)	0.003
LV EDVi, mL/m^2	11.7 ± 18.7	4.4 ± 15.0	0.183	7.5 ± 13.6	13.9 ± 22.2	0.224
LV ESVi, mL/m^2	4.4 (-0.9–9.9)	-0.7 (-5.9–4.1)	0.558	3.0 (-1.5–6.9)	5.3 (-2.4–14.7)	0.748
LV SVi, mL/m^2	5.3 (-2.3–12.1)	2.9 (-8.1–10.7)	0.315	3.2 (-4.9–12.2)	4.7 (-2.2–11.4)	0.446
Left atrial area, cm^2	-1.5 (-8.8–11.8)	-1.6 (-20.2–5.5)	0.614	-1.5 (-13.6–10.1)	-1.5 (-6.5–13.8)	0.559
LV EF, %	0.5 (-5.7–2.6)	1.9 (-4.8–11.7)	0.820	0.1 (-2.5–3.9)	-0.6 (-7.6–3.0)	0.755
LV circumferential strain, %	-0.2 (-2.2–1.9)	-0.2 (-1.8–1.9)	0.959	-0.4 (-2.2–1.6)	-0.1 (-2.2–2.6)	0.787
LV longitudinal strain, %	-0.5 (-3.0–1.1)	-0.1(-2.6–1.7)	0.671	-0.5 (-2.9–1.1)	-0.1 (-2.8–1.2)	0.284
LV radial strain, %	-0.9 (-2.1–1.4)	0.8 (-3.1–5.5)	0.817	1.1 (-2.4–5.5)	0.1 (-2.7–5.3)	0.299
LV basal segmental circumferential strain, %	0.2 ± 3.2	0.7 ± 2.8	0.579	-0.1 ± 2.9	0.7 ± 3.5	0.293
LV basal segmental longitudinal strain, %	-0.6 (-2.6–3.1)	-1.2 (-4.1–2.7)	0.880	-1.2 (-3.0–2.4)	-0.1 (-1.8–3.4)	0.334
LV basal segmental radial strain, %	2.5 ± 0.2	-0.6 ± 14.5	0.356	3.1 ± 10.4	0.3 ± 11.7	0.265
RV native T1, ms	2.5 (-117–63)	-27.0 (-138.0–60.0)	0.614	-27.0 (-118.0–43,5)	35.0 (-96.8–139.8)	0.130
RV ECV, %	-2.7 (-7.3–2.3)	3.6 (-1.9–4.6)	0.091	-2.9 (-8.7–1.1)	1.7 (-5.5–7.1)	0.017
RV massi, g/m^2	1.1 (-2.5–3.1)	0.7 (-2.6–2.9)	0.161	0.7 (-2.6–2.7)	1.2 (-2.4–3.1)	0.364
RV EDVi, mL/m^2	7.6 ± 21.6	4.3 ± 21.3	0.089	3.5 ± 20.1	11.3 ± 22.6	0.759
RV ESVi, mL/m^2	1.6 (-3.9–8.4)	4.3 (-4.9–6.7)	0.99	-0.2 (-5.0–7.0)	5.2 (-2.3–11.4)	0.408
RV SVi, mL/m^2	4.3 (-3.1–14.4)	-5.8 (-21.6–2.3)	0.007	2.3 (-3.3–14.5)	0.9 (-5.2–13.1)	0.646
Right atrial area, cm^2	-0.4 (-10.6–8.4)	0.8 (-18.9–13.0)	0.814	-2.1 (-12.4–8.2)	2.6 (-11.1–12.6)	0.746
RV EF, %	1.5 (-2.6–5.3)	-0.4 (-5.8–4.1)	0.009	1.7 (-1.6–4.7)	1.0 (-7.1–5.3)	0.243
RV circumferential strain, %	-0.5 (-2.4–1.4)	0.7 (-2.6–3.2)	0.271	-0.5 (-2.0–1.1)	0.3 (-3.1–1.8)	0.735
RV longitudinal strain, %	-1.6 (-3.1–1.1)	0.6 (-4.2–5.3)	0.082	-1.6 (-3.1–1.2)	-0.7 (-4.0–2.4)	0.798
RV radial strain, %	2.7 (-9.2–11.5)	4.4 (-4.5–11.1)	0.662	3.0 (-4.3–11.4)	2.7 (-10.1–10.9)	0.505

https://doi.org/10.3348/kjr.2023.0985

Table 3. Changes in serum biomarkers and CMR parameters according to response groups (continued)

Parameter	Hematologic response			Cardiac laboratory response		
	Superior response (n = 93)	Inferior response (n = 18)	*P*	Superior response (n = 59)	Inferior response (n = 52)	*P*
RV basal segmental circumferential strain, %	-0.5 (-3.2–3.0)	-0.4 (-3.5–3.9)	0.950	-0.5 (-2.6–3.1)	-1.0 (-4.7–3.0)	0.717
RV basal segmental longitudinal strain, %	-1.4 (-5.7–2.8)	1.1 (-4.5–3.6)	0.940	-0.8 (-4.4–2.6)	-1.6 (-6.1–3.2)	0.817
RV basal segmental radial strain, %	5.1 (-14.8–19.0)	16.1 (-14.6–29.8)	0.419	9.6 (-19.3–18.8)	-1.2 (-12.3–27.1)	0.950

Values are presented as mean ± standard deviation or median (interquartile range).
CMR = cardiac magnetic resonance, dFLC = difference between involved and uninvolved free light chains, cTnI = cardiac troponin I, NT-proBNP = N-terminal pro–B-type natriuretic peptide, LGE = late gadolinium enhancement, LV = left ventricle, ECV = extracellular volume fraction, massi = mass index, EDVi = end-diastolic volume index, ESVi = end-systolic volume index, SVi = stroke volume index, EF = ejection fraction, RV = right ventricle

following chemotherapy was more prominent and probably earlier than that of the left ventricle. Myocardial T2 levels increased over time, indicating that myocardial edema was associated with chemotherapy-induced cardiotoxicity. The integration of CMR parameters into response assessments may provide insights into individualized assessments and potentially influence the clinical management of AL-CA.

Supplement

The Supplement is available with this article at https://doi.org/10.3348/kjr.2023.0985.

Availability of Data and Material

The datasets generated or analyzed during the study are available from the corresponding author on reasonable request.

Conflicts of Interest

The authors have no potential conflicts of interest to disclose.

Author Contributions

Conceptualization: Yining Wang, Jian Li. Data curation: all authors. Formal analysis: Yubo Guo, Xiao Li. Funding acquisition: Yining Wang, Lu Lin. Investigation: Yubo Guo, Yajuan Gao. Methodology: Zhuoli Zhang, Jian Li, Yining Wang. Project administration: Yubo Guo, Xiao Li, Yajuan Gao, Ke Wan, Xi Yang Zhou. Resources: Jian Li, Yining Wang. Software: Yubo Guo. Supervision: Jian Li, Yining Wang. Validation: Jian Li, Yining Wang. Visualization: Yubo Guo, Xiao Li. Writing—original draft: Yubo Guo. Writing—review & editing: Zhuoli Zhang, Jian Li, Yining Wang.

ORCID IDs

Yubo Guo
https://orcid.org/0009-0009-7632-2667
Lu Lin
https://orcid.org/0000-0002-3261-6569
Long Jiang Zhang
https://orcid.org/0000-0002-6664-7224
Jian Li
https://orcid.org/0000-0002-4549-0694
Yining Wang
https://orcid.org/0000-0001-6441-2002

Funding Statement

This study was supported by the National Natural Science Foundation of China (Grant Nos. 82325026, 82020108018, and 82202134) and National High Level Hospital Clinical Research Funding (Grant Nos. 2022-PUMCH-B-027 and 2022-PUMCH-D-002).

Acknowledgments

The authors thank each of the study subjects for their participation.

REFERENCES

1. Gertz MA. Immunoglobulin light chain amyloidosis: 2022 update on diagnosis, prognosis, and treatment. *Am J Hematol* 2022;97:818-829
2. Falk RH, Alexander KM, Liao R, Dorbala S. AL (light-chain) cardiac amyloidosis: a review of diagnosis and therapy. *J Am Coll Cardiol* 2016;68:1323-1341

3. Kyle RA, Linos A, Beard CM, Linke RP, Gertz MA, O'Fallon WM, et al. Incidence and natural history of primary systemic amyloidosis in Olmsted County, Minnesota, 1950 through 1989. *Blood* 1992;79:1817-1822
4. Jaccard A, Comenzo RL, Hari P, Hawkins PN, Roussel M, Morel P, et al. Efficacy of bortezomib, cyclophosphamide and dexamethasone in treatment-naïve patients with high-risk cardiac AL amyloidosis (Mayo Clinic stage III). *Haematologica* 2014;99:1479-1485
5. Palladini G, Campana C, Klersy C, Balduini A, Vadacca G, Perfetti V, et al. Serum N-terminal pro-brain natriuretic peptide is a sensitive marker of myocardial dysfunction in AL amyloidosis. *Circulation* 2003;107:2440-2445
6. Fontana M, Pica S, Reant P, Abdel-Gadir A, Treibel TA, Banypersad SM, et al. Prognostic value of late gadolinium enhancement cardiovascular magnetic resonance in cardiac amyloidosis. *Circulation* 2015;132:1570-1579
7. Banypersad SM, Fontana M, Maestrini V, Sado DM, Captur G, Petrie A, et al. T1 mapping and survival in systemic light-chain amyloidosis. *Eur Heart J* 2015;36:244-251
8. Guo Y, Li X, Wang Y. State of the art: quantitative cardiac MRI in cardiac amyloidosis. *J Magn Reson Imaging* 2022;56:1287-1301
9. Gertz MA, Dispenzieri A. Systemic amyloidosis recognition, prognosis, and therapy: a systematic review. *JAMA* 2020;324:79-89
10. Palladini G, Dispenzieri A, Gertz MA, Kumar S, Wechalekar A, Hawkins PN, et al. New criteria for response to treatment in immunoglobulin light chain amyloidosis based on free light chain measurement and cardiac biomarkers: impact on survival outcomes. *J Clin Oncol* 2012;30:4541-4549
11. Messroghli DR, Moon JC, Ferreira VM, Grosse-Wortmann L, He T, Kellman P, et al. Clinical recommendations for cardiovascular magnetic resonance mapping of T1, T2, T2* and extracellular volume: a consensus statement by the Society for Cardiovascular Magnetic Resonance (SCMR) endorsed by the European Association for Cardiovascular Imaging (EACVI). *J Cardiovasc Magn Reson* 2017;19:75
12. Lin L, Li X, Feng J, Shen KN, Tian Z, Sun J, et al. The prognostic value of T1 mapping and late gadolinium enhancement cardiovascular magnetic resonance imaging in patients with light chain amyloidosis. *J Cardiovasc Magn Reson* 2018;20:2
13. Yim D, Riesenkampff E, Caro-Dominguez P, Yoo SJ, Seed M, Grosse-Wortmann L. Assessment of diffuse ventricular myocardial fibrosis using native T1 in children with repaired tetralogy of fallot. *Circ Cardiovasc Imaging* 2017;10:e005695
14. Li X, Huang S, Han P, Zhou Z, Azab L, Lu M, et al. Nonenhanced chemical exchange saturation transfer cardiac magnetic resonance imaging in patients with amyloid light-chain amyloidosis. *J Magn Reson Imaging* 2022;55:567-576
15. Chamling B, Bietenbeck M, Drakos S, Korthals D, Vehof V, Stalling P, et al. A compartment-based myocardial density approach helps to solve the native T1 vs. ECV paradox in cardiac amyloidosis. *Sci Rep* 2022;12:21755
16. Leone O, Longhi S, Quarta CC, Ragazzini T, De Giorgi LB, Pasquale F, et al. New pathological insights into cardiac amyloidosis: implications for non-invasive diagnosis. *Amyloid* 2012;19:99-105
17. Martinez-Naharro A, Patel R, Kotecha T, Karia N, Ioannou A, Petrie A, et al. Cardiovascular magnetic resonance in light-chain amyloidosis to guide treatment. *Eur Heart J* 2022;43:4722-4735
18. Martinez-Naharro A, Abdel-Gadir A, Treibel TA, Zumbo G, Knight DS, Rosmini S, et al. CMR-verified regression of cardiac AL amyloid after chemotherapy. *JACC Cardiovasc Imaging* 2018;11:152-154
19. Fontana M, Martinez-Naharro A, Chacko L, Rowczenio D, Gilbertson JA, Whelan CJ, et al. Reduction in CMR derived extracellular volume with patisiran indicates cardiac amyloid regression. *JACC Cardiovasc Imaging* 2021;14:189-199
20. Bodez D, Ternacle J, Guellich A, Galat A, Lim P, Radu C, et al. Prognostic value of right ventricular systolic function in cardiac amyloidosis. *Amyloid* 2016;23:158-167
21. Sengupta PP, Tajik AJ, Chandrasekaran K, Khandheria BK. Twist mechanics of the left ventricle: principles and application. *JACC Cardiovasc Imaging* 2008;1:366-376
22. Cohen OC, Ismael A, Pawarova B, Manwani R, Ravichandran S, Law S, et al. Longitudinal strain is an independent predictor of survival and response to therapy in patients with systemic AL amyloidosis. *Eur Heart J* 2022;43:333-341
23. Cuddy SAM, Jerosch-Herold M, Falk RH, Kijewski MF, Singh V, Ruberg FL, et al. Myocardial composition in light-chain cardiac amyloidosis more than 1 year after successful therapy. *JACC Cardiovasc Imaging* 2022;15:594-603
24. Zheng Y, Huang S, Xie B, Zhang N, Liu Z, Tse G, et al. Cardiovascular toxicity of proteasome inhibitors in multiple myeloma therapy. *Curr Probl Cardiol* 2023;48:101536
25. Kim J, Hong YJ, Han K, Kim JY, Lee HJ, Hur J, et al. Chemotherapy-related cardiac dysfunction: quantitative cardiac magnetic resonance image parameters and their prognostic implications. *Korean J Radiol* 2023;24:838-848
26. Edwards CV, Rao N, Bhutani D, Mapara M, Radhakrishnan J, Shames S, et al. Phase 1a/b study of monoclonal antibody CAEL-101 (11-1F4) in patients with AL amyloidosis. *Blood* 2021;138:2632-2641
27. Cuddy SAM, Bravo PE, Falk RH, El-Sady S, Kijewski MF, Park MA, et al. Improved quantification of cardiac amyloid burden in systemic light chain amyloidosis: redefining early disease? *JACC Cardiovasc Imaging* 2020;13:1325-1336